

J. Am. Chem Soc. 117, 6064-6070 (1995).

Exchange Rates of Internal Water Molecules in Proteins Measured Using Pulsed Field Gradients

Volker Dötsch[¶] and Gerhard Wider*

*Institut für Molekularbiologie und Biophysik,
Eidgenössische Technische Hochschule–Hönggerberg,
CH–8093 Zürich, Switzerland*

Keywords: protein hydration, pulsed magnetic field gradient, water exchange rate, NMR

* : author to whom correspondence should be addressed

¶ : present address: Dep. of Biological Chemistry and Molecular Pharmacology, Harvard Medical School, Boston, Massachusetts 02115.

Abstract

Observation of individual hydration water molecules located in the solvent-inaccessible core of globular proteins by nuclear magnetic resonance (NMR) spectroscopy showed that these have identical ^1H chemical shifts as the bulk water, implicating exchange-averaging of the shifts in the two environments. Measurement of the water exchange rates for the internal hydration sites is of interest since these can be directly related to the frequency of internal motions of the protein. This paper describes measurements of the water exchange-rates with an experimental scheme based on the use of pulsed field gradients. The previously established lower limit of $k_{\text{ex}} > 50 \text{ s}^{-1}$ for the exchange rates of the four internal water molecules in the basic pancreatic trypsin inhibitor could thus be raised to $k_{\text{ex}} > 1 \cdot 10^3 \text{ s}^{-1}$, with an upper limit of $k_{\text{ex}} < 1 \cdot 10^9 \text{ s}^{-1}$ established by previous investigations.

1. Introduction

Although it is characteristic for the folded state of polypeptide chains in globular proteins that the solvent is excluded from the molecular core, a small number of "interior hydration water molecules" is usually observed.² These are typically completely shielded from the bulk solvent, form hydrogen bonds with surrounding polar groups of the polypeptide chain, and are thus an integral part of the protein architecture. Similar "interior" waters have been reported for the intermolecular interface in multimolecular complexes with proteins, for example, in protein–DNA complexes.^{3,4} Hydration studies using NMR¹ spectroscopy, which are based on the observation of ¹H–¹H NOEs between the protein and the bound water molecules⁵, showed that two classes of hydration water molecules with qualitatively different characteristics can be distinguished in aqueous protein solutions:^{6–8} (i) "Structural", interior hydration waters for which the cross relaxation of the water protons with nearby polypeptide protons is in the slow motional regime, with opposite sign of the cross relaxation rate constants in the laboratory frame of reference, σ^{NOE} , and in the rotating frame, σ^{ROE} , which have life times with respect to exchange with the bulk water of $\tau_{\text{ex}} > 10^{-9}$ s⁷. (ii) Surface hydration waters with exchange life times in the approximate range 10^{-11} to 10^{-10} s,^{6,8,9} for which σ^{NOE} and σ^{ROE} have the same sign.⁶ Because of the long residence times on the NOE time scale, interior hydration waters give much more intense NOEs with the protein than the surface hydration waters, and therefore NMR observations of interior waters have been reported for numerous different systems.^{4,5,10} In all cases the same ¹H chemical shifts were observed for the interior waters and the bulk water, which was shown with the use of paramagnetic shift reagents to be due to exchange averaging,⁷ and a lower limit of $k_{\text{ex}} > 50$ s⁻¹ was established for the exchange of interior waters in the basic pancreatic trypsin inhibitor (BPTI) (Figure 1). More recently NMR methods using pulsed field gradients^{11, 12} have been proposed for the measurement of exchange rates. However, measurements of fast exchange rates in the range of 10^3 s⁻¹ have not been possible so far. Recent advances in gradient spectroscopy have overcome some of the limiting factors of such measurements^{13, 14}.

Measurements of exchange rates with the use of pulsed field gradients are based on the fact, that molecules with different translational diffusion constants can be distinguished by the

different decrease of their signal intensities.^{11, 15} When water molecules are transiently bound to macromolecules, their apparent diffusion constant will become the weighted average of the diffusion constants of free water and the hydrated protein. This difference in the apparent diffusion constants can lead to different decay rates of the signal intensity in a PFG-based experiment for the water molecules in the bound and the free state, whereby the difference of the two decay rates depends on the exchange rate between the two states. The use of these principles for studies of protein hydration has recently been proposed.¹² We present an alternative experimental scheme, which allows to determine a more precise lower limit for the water exchange rate constants in BPTI. Although the following discussion concentrates on the measurement of the exchange rates of internal water molecules, the same pulse sequence and the same model calculations (see below) can be used for the determination of exchange rates, e.g. of fast exchanging hydroxyl or amide protons with the bulk water.

2. The NMR Experimental Scheme Used for the Exchange Measurements

Since the hydration water chemical shift coincides with that of the bulk water⁷ the decay of the signal intensity of the bound waters must be observed via the decay of the intensity of the NOE cross peaks with protons of the protein. The pulse sequence for exchange spectroscopy¹¹ used here was modified with self-compensating "PFG sandwiches"¹³, which are applied before and after the mixing time, τ_m , and in the way the water signal is suppressed (Figure 2). As described previously¹³, the use of the PFG sandwiches reduces the recovery time after the application of the gradients and ensures refocusing of the chemical shift evolution. To further reduce magnetic field instabilities caused by switching on and off the gradients, the individual gradient amplitudes have a sine squared dependence during the first quarter and a cosine squared dependence during the last quarter. An additional PFG in the middle of the mixing time eliminates coherences present after the second $\frac{\pi}{2}$ -pulse. Water suppression is achieved by a pair of orthogonal trim pulses separated by a short delay, τ_1 ^{16,17}. The first trim pulse has the additional effect of ensuring an absorptive lineshape at the expense of a

loss in sensitivity by a factor of 2 compared to NOESY without use of gradients for coherence selection¹⁴.

For the determination of the exchange rates, a series of [¹H,¹H]-NOESY spectra with increasing gradient strength from 1.8 to 180 Gauss/cm was measured. The cross section along ω_2 of these spectra taken at the ω_1 chemical shift of water contains the NOE cross peaks between the internal water molecules and protons of the protein⁵. Due to the application of the extremely strong gradients many cross peaks in this cross section, especially in the high field shifted part, were distorted by strong t_1 noise bands and could therefore not be taken into account. Thus, the well resolved and undistorted cross peaks to the amide protons of Cys 14 and Gly 36, which manifest interaction with the single water molecule W122^{5,18} of BPTI were integrated. Additionally the cross peak to the amide proton of Lys 41, which is caused by interaction with the cluster of the three water molecules W111, W112 and W113^{5,18} was used. The locations of the four internal water molecules in the crystal structure of BPTI are shown in Figure 1. Examples of cross sections measured at different gradient strengths are given in Figure 3. In the data analysis we have investigated the exchange rates for the single water molecule W122 and for the water cluster separately. The data obtained are shown in Figure 4 as ratios of the integrals at a certain gradient strength and the integrals of the reference measurement at 1.8 Gauss/cm (see section below).

3. Data Analysis

As a basis for the interpretation of the measurements with the sequence of Figure 2, we compared the experimental data with calculated data. Based on the model described in the appendix the NOE-build-up of the cross peak volume, V , during τ_m can be described by eq 1,

$$V = \frac{\sigma M^0}{(k_{ex} - k_b)} \left[\frac{k_{ex}}{k_b} (1 - \exp(-k_b \tau_m)) - \frac{k_b}{k_{ex}} (1 - \exp(-k_{ex} \tau_m)) \right] \quad (1)$$

where σ is the cross relaxation rate, k_{ex} the exchange rate of the internal water molecules and M^0 the average magnetization per water molecule at the beginning of the experiment. If we assume that self-diffusion of the bulk water and exchange of the internal water molecules during the application of the gradients can be neglected, M^0 is the same for all water molecules also at the start of the mixing time, τ_m . k_b is the rate constant for the decay of the bulk water magnetization caused by the application of the gradients. Its dependence on the experimental parameters is given in eq A4 of the appendix.

If k_{ex} becomes larger than k_b , the apparent diffusion constant of the internal water molecules approaches the diffusion constant of the bulk water. As a consequence the NOE build-up curves for the internal water molecules reach a limit, V_L , which is a function of k_b , but not of k_{ex} any more. In this fast exchange regime the NOE build-up curves for different exchange rates can no longer be distinguished and only a lower limit of the exchange rate can be determined. We have compared our experimental data also with this function V_L , which follows from eq 1 for the case $k_{ex} \gg k_b$:

$$V_L = \frac{M^0 \sigma}{k_b} (1 - \exp(-k_b \tau_m)) \quad (2)$$

Although the diffusion constant of the protein is one order of magnitude smaller than the one of the bulk water, the signal attenuation caused by diffusion of the protein during τ_m has for a quantitative interpretation of the exchange measurements also to be considered. This can be achieved by multiplying V with an exponential function, which describes the decay of the pro-

tein magnetization (eq A7 in the appendix). However, the intensity of the cross peaks in the spectrum might not be attenuated by the diffusion of the protein alone, but also by residual instabilities of the magnetic field caused by the gradients. Therefore the experimental data were scaled such that the intensity of intraresidual cross peaks became the same for all spectra measured at different gradient strengths. Thus the theoretical curves could be calculated using eq 1. To illustrate the amount of loss of magnetization due to protein diffusion, Figure 5 shows two sections of NOESY-spectra, measured at a gradient strength of 1.8 G/cm and 180 G/cm. For a further illustration, cross sections of the two NOESY spectra are compared in Figure 6. These figures show, that the loss of magnetization is 34% at a gradient strength of 180 G/cm, which corresponds to a diffusion constant of the protein in a 20 mM solution at 277 K of $4.7 \times 10^{-7} \text{ cm}^2 \text{ s}^{-1}$.

Equation 1 is a function of the cross relaxation rate σ and the magnetization M^0 of the water molecules at the beginning of the experiment. These quantities can, however, be eliminated by dividing eq 1 by

$$V^0 = M^0 \sigma \tau_m \quad (3)$$

which describes the build-up of the cross peaks without application of gradients in the initial rate approximation. In order to make measuring conditions for this reference NOESY spectrum as similar as possible to the measuring conditions of the PFG- ^1H , ^1H -NOESY series, we used a spectrum measured with 1% of the maximum gradient strength (1.8 Gauss/cm) to determine the reference V^0 . In the following the results will be discussed on the basis of these "normalized volumes", V_n :

$$V_n = \frac{V}{V^0} = \frac{1}{(k_{ex} - k_b) \tau_m} \left[\frac{k_{ex}}{k_b} (1 - \exp(-k_b \tau_m)) - \frac{k_b}{k_{ex}} (1 - \exp(-k_{ex} \tau_m)) \right] \quad (4)$$

For V_L the corresponding normalized limit function, V_{nL} , is obtained by dividing eq 2 by eq 3.

The difference between the two functions, V_n and V_{nL} , will be referred to as Δ_v :

$$\Delta_v = V_n - V_{nL} = \frac{1}{(k_{ex} - k_b)\tau_m} \left[(1 - \exp(-k_b\tau_m)) - \frac{k_b}{k_{ex}} (1 - \exp(-k_{ex}\tau_m)) \right] \quad (5)$$

Figure 4 shows the experimental normalized volumes, V_n , for the cross peak of Lys 41, which is caused by magnetization transfer from the cluster of three waters and for the sum of the cross peaks of Cys 14 and Gly 36, which result from interaction with the single water W122 (Figure 1). Furthermore, two curves calculated for an exchange rate of $k_{ex} = 10^3 \text{ s}^{-1}$ and 10^2 s^{-1} and the normalized limit function, V_{nL} , are shown. The experimental data for both types of cross peaks closely follow the curve calculated for an exchange rate of 10^3 s^{-1} . However, the difference Δ_v between V_n for $k_{ex}=10^3 \text{ s}^{-1}$ and V_{nL} is smaller than the estimated error of the experiment ($\pm 500 \text{ s}^{-1}$). As a consequence we cannot measure the actual exchange rate, but can only determine a lower limit. This lower limit is 10^3 s^{-1} for both, the single water molecule W122 and the cluster of the three waters W111, W112 and W113 (Figure 1).

For the calculation of the functions V_n and V_{nL} in Figure 4 diffusion of the bulk water molecules and exchange of the internal water molecules during the application of the PFG sandwiches were neglected. For residence times of the internal water molecules shorter than 1 ms and actual gradient lengths of 1 to 2 ms this assumption is not justified. As a consequence, the magnetization at the beginning of τ_m is not the same for the water molecules in the interior of the protein and in the bulk and is for both different from the magnetization at the beginning of the pulse sequence, M^0 . Therefore eq 1 has to be replaced by eq 6, which describes the NOE-build-up with the boundary condition, that M^0 is replaced by the magnetization of the bulk water at the beginning of τ_m , M_b^0 , or by the corresponding magnetization of the internal water molecules, M_i^0 :

$$V = \frac{\sigma M_b^0 k_{ex}}{k_{ex} - k_b} \left[\frac{1}{k_b} (1 - \exp(-k_b\tau_m)) - \frac{1}{k_{ex}} (1 - \exp(-k_{ex}\tau_m)) \right] + \frac{\sigma M_i^0}{k_{ex}} (1 - \exp(-k_{ex}\tau_m)) \quad (6)$$

Additionally M^0 has to be replaced in eq 2 by M_b^0 . The exact calculation of the influence of

exchange during the gradient time, involves the determination of integrals, which cannot be analytically solved (see appendix). However, it can be estimated, that with the parameters used in the experiments described in this paper, the maximum reduction of the cross peak intensity at the highest gradient strength is 10% (see appendix). This reduction is within the error limits of the measurement. Improvements of the hardware and the experimental setup as discussed below, will make the determination of actual exchange rates possible. Therefore we include here a qualitative description, how different exchange rates will influence the result relative to the calculations without explicitly taking the exchange during the gradients into account. If the exchange is very fast, the magnetization of the internal water molecules will closely follow the magnetization of the bulk water molecules. This means M_i^0 and M_b^0 , will be scaled down relative to M^0 . Consequently also Δ_v will be reduced. In case the exchange rate is slow relative to k_b , M_i^0 and M_b^0 differ at the beginning of τ_m and Δ_v gets less reduced or even increases relative to the value of Δ_v calculated neglecting the influence of exchange during the gradient period.

4. Comparison with an Alternative Experimental Scheme

Recently a different pulse sequence for measuring the exchange rates of internal water molecules has been proposed¹². In the following, this alternative experimental scheme will be referred as method II, and the one introduced in the preceding section as method I.

The two pulse sequences differ in the position of the gradient pulses. Instead of having the NOESY mixing time embedded between the gradients, the refocusing gradient in method II directly precedes τ_m . To be able to compare the two schemes, we have calculated the theoretical NOE build-up for method II. Equation 7 describes the build-up of the NOE cross peak volumes between the internal water molecules and the protein.

$$V = M_b \sigma \tau_m + \sigma \frac{M^0 - M_b}{k_{ex}} (1 - \exp(-k_{ex} \tau_m)) \quad (7)$$

Again it was assumed, that no exchange of the internal water molecules occurs during the

application of the gradients. The corresponding limit function for fast exchange, V_L , is:

$$V_L = M_b \sigma \tau_m = M^o \exp\left(-k_b \left(T_G - \frac{\delta_g}{3}\right)\right) \sigma \tau_m \quad (8)$$

in which T_G denotes the time between the start of the first PFG and the start of the second one¹⁵. The normalization of the two equations can be done as described above, leading to eq 9 for the difference Δ_v for method II:

$$\Delta_v = V_n - V_{nL} = \frac{1 - \exp(-k_b(T_G - \delta_g/3))}{k_{ex} \tau_m} (1 - \exp(-k_{ex} \tau_m)) \quad (9)$$

The main difference between the two methods is the fact, that in method II the magnetization of the bulk water molecules is not a function of the mixing time. Figure 4 shows the theoretical dependence of the cross peak volumes on the gradient strength for method II in addition to those of method I. Three exchange rates k_{ex} were used, 10^3 s^{-1} , 10^2 s^{-1} and indefinitely fast exchange, which corresponds to the normalized limit function, V_{nL} . The graphs for method II were calculated by dividing eq 7 by eq 3. Comparing the two sets of curves it is clear, that the intensity of the cross peaks is larger for method II. However, for the determination of the exchange rates, the difference Δ_v between V_n and V_{nL} is relevant. This difference is about three times larger for method I compared to II. If exchange during the application of the gradients is considered Δ_v will get smaller again. For method II, M^o in eq 7 has to be replaced by M_1^o . From eq 7 and eq 8 it is obvious, that Δ_v is proportional to the difference of M_1^o and M_b . Therefore a reduction in M_1^o due to exchange decreases Δ_v . Furthermore, the gradient period, which is relevant for exchange is in method II twice as long as in method I. This makes the second experimental scheme less suitable for measurements in the fast exchange regime. On the other hand, in method II no signal is lost due to diffusion of the protein during the mixing time τ_m and due to the use of gradients for coherence selection. In summary, method II seems to be superior for moderate exchange rates and if the signal-to-noise ratio is a limiting factor. This is for example the case in investigations of dilute solutions of small and rather fast diffusing molecules as binding partners for the water or other molecules.

5. Discussion

The comparison of our experimental data with the results from the calculation using method I shows (Figure 4), that the actual exchange of the internal water molecules is equal to or faster than the upper limit for the measurement of exchange rates with the currently available maximal gradient strength of 180 G/cm. The results presented in Figure 4 allow to lower the limit of the exchange rate of the internal water molecules in BPTI with the bulk water by a factor of 20 to 10^3 s^{-1} , as compared to 50 s^{-1} that could be estimated using paramagnetic shift reagents⁸. This limit could be established for both, the cluster of three water molecules, which is partly surface accessible and the completely buried single water molecule W122 (Figure 1). This shows, that motions with amplitudes of approximately 0.15 nm must occur with a frequency of at least 10^3 s^{-1} even in the core of a small protein.

The experiments described in this paper are technically demanding. Very high gradient field strength of 180 G/cm or more are necessary to measure exchange rates in the range of 10^3 s^{-1} , but with increasing gradient strength the residual magnetic field instabilities causing t_1 -noise bands and magnetization losses due to protein diffusion become worse. Furthermore, also the cross peak intensity of the NOEs between water and protein decreases with increasing gradient strength. To compensate at least a part of these magnetization losses the mixing time τ_m has to be optimized. In principle the cross peak volume increases with τ_m , however, with longer mixing times the magnetization of the internal water molecules decreases. Therefore the signal-to-noise ratio will reach a maximum at a certain mixing time. As mentioned above, not the signal volume itself but the difference function Δ_v is the crucial parameter for the determination of fast exchange rates. For long mixing times Δ_v decreases approximately with $1/\tau_m$ (eq 5). For the measurement of very fast exchange rates, a short mixing time has therefore to be chosen. Obviously, for measurements of fast exchange rates a compromise between

maximizing Δ_v and optimizing V_n has to be found. On the basis of these considerations we have chosen a mixing time of 30 ms for the experiments used to determine the exchange rate of internal water molecules in BPTI.

In the following we will discuss improvements of the experimental setup, which will make the determination of faster exchange rates possible, if the signal-to-noise ratio is not the limiting factor. First the difference function Δ_v has to be analysed in more detail. Figure 7 shows Δ_v as a function of the mixing time, calculated for both methods for an exchange rate of 10^3 s^{-1} and a gradient strength of 180 Gauss/cm. Except for unreasonable short mixing times Δ_v for method I is always larger. The function Δ_v for method II decays very fast and it will be difficult to obtain a precise value for Δ_v from the experiment. Judging from our experimental data a difference of 10% between V_n and V_{nL} , i.e. a value of 0.1 for Δ_v in Figure 7, at a residual intensity of 15 - 20% of the reference cross peaks seems significant to be used for the determination of the actual exchange rate. Figure 7 shows, that this difference is reached with method I at a mixing time of 10 ms. With these measuring conditions, determination of exchange rates in the range of 10^3 s^{-1} will be possible. For method II a mixing time of only 3 ms would have to be chosen, making it extremely difficult to use method II for the measurement of fast exchange rates. At these short mixing times the decay of the magnetization due to exchange during the application of the gradients can not be neglected, but has to be treated quantitatively.

The limit of the exchange rate, which is measurable under given conditions is determined by the ratio of k_{ex} and k_b , i.e. the magnetization of the bulk water has to be destroyed in a much shorter time, than the inverse of the exchange rate, k_{ex} . The goal to obtain a larger value for k_b can be reached in principle by increasing one or several of the following parameters (eq A4): the gradient length δ , the diffusion constant D_b of the bulk water, the gradient strength G_r . Choosing a larger δ results in a reduction of Δ_v and in a loss of cross peak intensity due to exchange during the application of the gradients. Therefore δ and the recovery time after the gradient have rather to be decreased than increased. The next parameter, D_b , can be increased by measuring at higher temperatures or by decreasing the viscosity of the solution. Higher temperature, however, will accelerate the exchange resulting in the same detrimental

effects as longer δ delays. Changing the viscosity of the solution substantially requires measurements in dilute solutions leading to a loss in signal-to-noise that more than outweighs the effects of a faster diffusion. Therefore the most appropriate way for the measurement of very fast exchanging water molecules in the interior of proteins seems to be the use of shorter and stronger gradients, reduction of the recovery time after the application of a gradient, reduction of the mixing time and simultaneous application of x- y- and z-gradients. With such an improved gradient hardware, measurements of residence times of internal water molecules in the submillisecond range will be possible in the future.

6. Experimental Section

The exchange measurements described in this paper were performed with a 20 mM solution of BPTI in 90% H_2O /10% D_2O at pH 3.5 and a sample temperature of $T=277$ K. [^1H , ^1H]-NOESY spectra using the pulse sequence shown in Figure 2 were measured on a Bruker AMX-500 NMR spectrometer equipped with shielded gradient coils and a Bruker 30 A gradient amplifier. Pulsed field gradients (PFGs) were applied as self-compensating sandwiches.¹³ The duration δ of a single PFG was 750 μs . The shape of the gradients was modified in the first quarter with a \sin^2 and in the last quarter with a \cos^2 function. The delay between PFG and the following $\frac{\pi}{2}$ or spinlock-pulse was 100 μs , and the delay between PFGs and π pulse in the PFG sandwich was 10 μs . Measurements were carried out at gradient strengths, G_r , of 1.8, 15, 30, 45, 72, 90, 108, 144 and 180 Gauss/cm. Residual coherences during τ_m were eliminated by the single PFG used as a "homospoil" in the middle of τ_m with a length, δ_h , of 2 ms and a strength of 18 Gauss/cm. The gradient unit was disconnected from the gradient coil before the start of the acquisition and reconnected immediately before the first $\frac{\pi}{2}$ -pulse of the experiment with the help of a Bruker B-GB 30 blanking unit. The mixing time, τ_m , was 30 ms. Water suppression was achieved by two orthogonal trim pulses with length $SL_1=1.7$ ms and $SL_2=2.6$ ms. The delay τ_1 between SL_1 and SL_2 was set to 135 μs . 140 complex points were measured in t_1 , each with 128 scans. The final complex time domain data matrix had a size of

140 x 1024 points corresponding to $t_{1\max} = 28$ ms and $t_{2\max} = 147$ ms. Quadrature detection in t_1 was obtained by altering the phase Φ_1 according to States-TPPI¹⁹. For obtaining a better resolution, the spectra were folded in the indirect dimension ω_1 . The spectral width in ω_1 was 5000 Hz and in ω_2 6900 Hz. Spectra were processed with the software package Prosa²⁰ without baseline correction in ω_2 . Zero-filling was applied in t_1 to 256 complex points. Using the software UXNMR²¹ the 1D cross sections along ω_2 , taken at the ω_1 chemical shift of water were baseline-corrected manually and the cross peaks between the internal water molecules and the backbone amide protons of Cys 14, Gly 36 and Lys 41 were integrated. The exponential function in eq A7 was determined from 20 intraresidual cross peaks of the protein. For the calculation of the graphs for different exchange rates (Figure 4), the diffusion constant of the bulk water in a 20 mM solution of BPTI was used ($1.0 \times 10^{-5} \text{ cm}^2 / \text{s}$)¹³.

Acknowledgments

We thank Prof. K. Wüthrich for reading the manuscript, his helpful comments and his encouragement. We are grateful to SPECTROSPIN AG (Fällanden, Switzerland) for providing a self-shielded gradient accessory. Financial support was obtained from the Kommission zur Förderung der wissenschaftlichen Forschung (project 2223.1).

REFERENCES

1. Abbreviation used: NMR, nuclear magnetic resonance; σ^{NOE} , cross relaxation rate in the laboratory frame; σ^{ROE} , cross relaxation rate in the rotating frame; NOE, nuclear Overhauser enhancement; BPTI, basic pancreatic trypsin inhibitor; PFG, pulsed field gradient; NOESY, two-dimensional NOE spectroscopy; SL, spin lock; TPPI, time-proportional phase incrementation.
2. Bernstein, F.C.; Kotzle, T.F.; Williams, G.J.B.; Meyer, E.F., Jr.; Brice, M.D.; Rodgers, J.R.; Kennard, O.; Shimamouchi, T.; Tasumi, M. *J. Mol. Biol.* **1977**, *112*, 535-542.
3. Otwinowski, Z.; Schevitz, R. W.; Zhang, R. G.; Lawson, C. L.; Joachimiak, A.; Marmorstein, R. Q.; Luisi, B. F.; Sigler, P. B. *Nature* **1988**, *335*, 321-329.
4. (a) Qian, Y. Q.; Otting, G.; Wüthrich, K. *J. Am. Chem. Soc.* **1993**, *115*, 1189-1190.
(b) Billeter, M.; Qian, Y. Q.; Otting, G.; Müller, M.; Gehring, W. J.; Wüthrich, K. *J. Mol. Biol.* **1993**, *234*, 1084-1093.
5. Otting, G.; Wüthrich, K. *J. Am. Chem. Soc.* **1989**, *111*, 1871-1875.
6. Otting, G.; Liepinsh, E.; Wüthrich, K. *Science* **1991**, *254*, 974-980.
7. Otting, G.; Liepinsh, E.; Wüthrich, K. *J. Am. Chem. Soc.* **1991**, *113*, 4363-4364.
8. Otting, G.; Liepinsh, E.; Wüthrich, K. *J. Am. Chem. Soc.* **1992**, *114*, 7093-7095.
9. Brunne, R. M.; Liepinsh, E.; Otting, G.; Wüthrich, K.; van Gunsteren, W. F. *J. Mol. Biol.* **1993**, *231*, 1040-1048.
10. (a) Clore, G. M.; Bax, A.; Wingfield, P. T.; Gronenborn, A. *Biochemistry* **1990**, *29*, 5671-5675; (b) Gerothanassis, I. P.; Birdsall, B.; Bauer, C. J.; Frenkiel, T. A.; Feeney, J. *J. Mol. Biol.* **1992**, *226*, 549-554; (c) Xu, R. X.; Meadows, R. P.; Fesik, S. W. *Biochemistry* **1993**, *32*, 2473-2480.
11. Moonen, C. T. W.; van Gelderen, P.; Vuister, G. W.; van Zijl, P. C. M. *J. Magn. Reson.* **1992**, *97*, 419-425.
12. Kriwacki, R.W.; Hill, R.B.; Glanagan, J.M.; Caradonna, J.P.; Prestegard, J.H. *J. Am. Chem. Soc.* **1993**, *115*, 8907-8911.
13. Wider, G.; Dötsch, V.; Wüthrich, K. *J. Magn. Reson. A* **1994**, *108*, 255-258.
14. Dötsch, V.; Wider, G.; Wüthrich, K. *J. Magn. Reson. A* **1994**, *109*, 263-264.
15. Stejskal, E. O.; Tanner, J. E. *J. Chem. Phys.* **1965**, *42*, 288-292.

16. Messerle, B.A.; Wider, G.; Otting, G.; Weber, C.; Wüthrich, K. *J. Magn. Reson.* **1989**, *85*, 608-613.
17. Otting, G.; Liepinsh, E.; Farmer II, B.T.; Wüthrich, K. *J. Biomol. NMR* **1991**, *1*, 209-215.
18. Wlodawer, A.; Walter, J.; Huber, R.; Sjölin, L. *J. Mol. Biol.* **1984**, *180*, 301-329.
19. Marion, D.; Ikura, K.; Tschudin, R.; Bax, A. *J. Magn. Reson.* **1989**, *85*, 393-399.
20. Güntert, P.; Dötsch, V.; Wider, G.; Wüthrich, K. *J. Biomol. NMR* **1992**, *2*, 619-629.
21. Bruker Analytische Messtechnik GmbH *UXNMR*. Messen und Verarbeiten von NMR Daten, Rheinstetten, **1991**.
22. Neuhaus, D.; Williamson, M. *The Nuclear Overhauser Effect*, New York, VCH, **1989**.
23. Carr, H.; Purcell, E.M. *Phys. Rev.* **1954**, *94*, 630-638.
24. Stilbs, P. *Prog. NMR Spec.* **1987**, *19*, 1-45.

FIGURE CAPTIONS

Figure 1. Ribbon drawing of the crystal structure of BPTI. The location of the four internal waters is indicated with CPK-models of water molecules. The water molecules W111, W112 and W113 form a cluster, which is partly surface accessible, while W122 is isolated and completely buried. The locations of the residues Cys 14, Gly 36 and Lys 41 are indicated. NH_3^+ denotes the N-terminal end of the polypeptide chain and COO^- the C-terminus.

Figure 2. Experimental scheme for 2D [^1H , ^1H]-NOESY for PFG-based exchange rate measurements. t_1 is the evolution time, τ_m the NOESY mixing period, t_2 the acquisition time, δ the length of the PFGs, δ_h the length of the PFG used as a "homospoil" pulse during τ_m , SL_1 and SL_2 are spin-lock purge pulses for water suppression and τ_1 the chemical shift evolution delay between the two spin lock pulses. ^1H radiofrequency pulses are represented by vertical bars on the **rf** line, where $\pi/2$ - and π -pulses are indicated by thin and thick bars. PFGs are indicated by the shaded shapes on the line **g_z**. Each half-gradient in the two PFG sandwiches¹³ has a modified rectangular shape, with the first quarter having a \sin^2 - and the last quarter having a \cos^2 -dependence. Phase cycling: $\Phi_1 = 8(x), 8(-x)$; $\Phi_2 = 2\{2x, 2y, 2(-x), 2(-y)\}$; $\Phi_3 = 8\{x, (-x)\}$; $\Phi_4 = 4\{2(x), 2(-x)\}$; $\Phi_5 = 16(y)$; $\Phi_6 = 2\{4x, 4(-x)\}$; Φ_7 (receiver) = $2\{x, 2(-x), x\}, 2\{-x, 2x, -x\}$. Quadrature detection in t_1 is achieved by altering the phase Φ_1 according to States-TPPI¹⁹.

Figure 3. Series of cross sections through NOESY-spectra measured at different gradient strengths with the pulse sequence shown in Figure 2, taken at the ω_1 chemical shift of water. (A) $G_r = 1.8$ G/cm, (B) $G_r = 108$ G/cm, (C) $G_r = 180$ G/cm. The cross peaks selected for integration are labelled with the one letter code for amino acids.

The excitation profile along ω_2 leads to a sign inversion of all signals on one side of the water line. Therefore the low field regions of the cross sections were inverted for improved readability.

Figure 4. Comparison of calculated normalized cross peak intensities, V_n , as a function of gradient strength for different exchange rates with the measured data. The filled circles represent the sum of the integrals of the NOE cross peaks between the single water molecule W122 and the amide protons of Cys 14 and Gly 36 divided by the corresponding sum at 1% of the maximum gradient strength (see text). The open circles show the data for the cross peak between the backbone amide proton of Lys 41 and the cluster of three waters. Theoretical curves were calculated for both methods and for the exchange rates, k_{ex} , of 10^3 s^{-1} (— — — —) and 10^2 s^{-1} (· · · · · · · · · ·) with the experimental parameters. Additionally the normalized limit functions for fast exchange, V_{nL} , are shown (—————). The errors are estimated values, based on the integration of the peaks on the cross section. The error bars are indicated for the filled circles only. On the second horizontal scale the k_b values for the corresponding gradient strengths are given.

Figure 5. Expanded regions from two NOESY spectra, measured at different gradient strengths with the pulse sequence of Figure 2. From the ratios of the integrals of the intra-protein cross peaks, the scaling factors used for the correction of the protein diffusion were determined. The dashed line indicates the position of the cross sections shown in Figure 6. (A) $G_r = 1.8 \text{ G/cm}$, (B) $G_r = 180 \text{ G/cm}$.

Figure 6. Cross sections along the ω_2 axis through the two expanded regions shown

in Figure 5, taken at a ω_1 chemical shift of 3.78 ppm. The diffusion of the protein during τ_m results in reduction of the cross peak volume of 34% at 180 G/cm, which corresponds to a diffusion constant of the protein in a 20 mM solution at 277 K of $4.7 \times 10^{-7} \text{ cm}^2 \text{ s}^{-1}$.

Figure 7. Dependence on the mixing time of the difference Δ_v between the normalized cross peak intensities, V_n , and the normalized limit function for fast exchange, V_{nL} . The function Δ_v for method I is represented by the solid line (————) and for method II by the dashed line (- - - -). The curves were calculated for a gradient strength of 180 Gauss/cm, an exchange rate of 10^3 s^{-1} and the parameters used for the experiments described in the text. Exchange between the internal water molecules and the bulk water during the application of the gradients was neglected. For method I signal loss of the bulk water during the application of the gradients was not taken into account.

Appendix

This appendix describes the derivation of eq 1. Assuming, that the initial rate approximation is valid, the build-up of the NOE cross peak volumes, V , between internal water molecules and protein protons is given by eq A1²²,

$$\frac{dV}{d\tau_m} = \sigma M_i \quad (\text{A1})$$

where τ_m is the mixing time, σ the cross relaxation rate, and M_i the average magnetization per water molecule in the interior of the protein. Since the mixing time is embedded between two PFG sandwiches, M_i becomes a function of τ_m :

$$\frac{dM_i}{d\tau_m} = -k_{\text{ex}} M_i + k_{\text{ex}} M_b \quad (\text{A2})$$

k_{ex} denotes the exchange rate of the internal water molecules and M_b the average magnetization per water molecule of the bulk water. Signal loss due to relaxation is neglected, and M_b includes the surface hydration water, for which the exchange rates with the bulk water are several orders of magnitude faster than the detection limit of the present gradient method (see text).

The behaviour of M_b is described by the probability average integral^{23, 24}

$$M_b = M^0 \int_{-\infty}^{\infty} \cos\left(\gamma r \int_0^{2\delta} G(t) dt\right) \frac{1}{2\sqrt{\pi D_b \tau_m}} \exp\left(\frac{-r^2}{4D_b \tau_m}\right) dr \quad (\text{A3})$$

M^0 is the average magnetization of a water molecule at the beginning of the experiment, $G(t)$ is the time-dependent shape of the gradients, γ is the gyromagnetic ratio, δ is the length of the gradient, r is the displacement of a water molecule along the gradient axis during the mixing time, and D_b is the self-diffusion constant of water molecules in the bulk water. Making use of the fact that the integral of cosine squared and sine squared is equal to the integral of a rectan-

gle with the same amplitude, but half of the length, solving the integrals in eq A3 yields:^{11, 23}

$$M_b = M^0 \exp(-\gamma^2 G_r^2 \delta_g^2 D_b \tau_m) = M^0 \exp(-k_b \tau_m) \quad (\text{A4})$$

with G_r denoting the maximum strength of the gradient, δ_g the length of a rectangular shaped gradient with the same integral as the gradient used, and k_b being an abbreviation for the constants in the exponential.

After solving the differential equation in eq A2 the dependence of M_i on τ_m is given by:

$$M_i = \frac{k_{\text{ex}} M^0}{(k_{\text{ex}} - k_b)} \exp(-k_b \tau_m) - \frac{k_b M^0}{k_{\text{ex}} - k_b} \exp(-k_{\text{ex}} \tau_m) \quad (\text{A5})$$

Finally, using eq A1, the build-up of the cross peak volumes during τ_m is described by eq A6, which is identical with eq 1 given in the text:

$$V = \frac{\sigma M^0}{(k_{\text{ex}} - k_b)} \left[\frac{k_{\text{ex}}}{k_b} (1 - \exp(-k_b \tau_m)) - \frac{k_b}{k_{\text{ex}}} (1 - \exp(-k_{\text{ex}} \tau_m)) \right] \quad (\text{A6})$$

The decay of the magnetization caused by the diffusion of the protein during τ_m can be included by multiplying V with the exponential term of eq A4 in which the diffusion constant of the bulk water has been replaced by the diffusion constant of the protein, D_p . The corrected cross peak intensity, V_D , is thus given as

$$V_D = V \cdot \exp(-\gamma^2 G_r^2 \delta_g^2 D_p \tau_m) \quad (\text{A7})$$

Exchange during the application of the gradients causes a reduction of M^0 and leads therefore to a reduced intensity of the cross peaks (eq A6). The rate of the magnetization loss is described by eq A8:

$$\frac{dM_i}{d\delta_g} = -k_{\text{ex}} M_i + k_{\text{ex}} M^0 \exp\left(-\gamma^2 G_r^2 D_b \delta_g^3 / 3\right) \quad (\text{A8})$$

The integration of eq A8 cannot be done analytically. However, the maximum reduction in the intensity of the cross peaks can be estimated for the case where the decay of the internal water magnetization is as fast as the decay for the bulk water. In this limit one can calculate, that for a gradient strength of 180 G/cm and a gradient length of 1.125 ms, the loss of the cross peak intensity will be about 10%.

At high gradient strengths and high exchange rates k_{ex} , the cross peak volume, V , reaches a plateau after a few milliseconds. During the rest of the mixing time, this magnetization decays, e.g. by back transfer to internal water molecules. In this case the initial rate approximation of eq A1 is no longer valid. Including back transfer to the internal waters, eq A1 has to be changed to:

$$\frac{dV}{d\tau_m} = \sigma M_i - \sigma M_p \quad (\text{A9})$$

in which M_p is the magnetization transferred from the internal waters to the protein. The increase in the magnetization of M_i due to this back transfer can be neglected. The solution of eq A9 can be written as

$$V = \frac{\sigma M^0}{(k_{ex} - k_b)} \left[\frac{k_{ex}}{k_b - \sigma} (\exp(-\sigma\tau_m) - \exp(-k_b\tau_m)) - \frac{k_b}{k_{ex} - \sigma} (\exp(-\sigma\tau_m) - \exp(-k_{ex}\tau_m)) \right] \quad (\text{A10})$$

In the limit of fast exchange and high gradient strengths, eq A10 can be simplified:

$$V = \frac{\sigma M^0}{(k_{ex} - k_b)} \left[\frac{k_{ex}}{k_b} - \frac{k_b}{k_{ex}} \right] \exp(-\sigma\tau_m) = V_{ira} \exp(-\sigma\tau_m) \quad (\text{A11})$$

V_{ira} is the build-up of the cross peak volumes in the initial rate approximation (eq A6). For the reference cross peak volumes, V^0 , the solution of eq A9 can be written in a good approximation as:

$$V^0 = M^0 \sigma \tau_m \exp(-\sigma\tau_m) \quad (\text{A12})$$

The normalization process introduced in the text involves the formation of the ratio of eq A11 and eq A12 which leads to the cancellation of the exponential term. The ratio is the same as for the calculation with the initial rate approximation. The errors introduced by the approximations in the derivation of the equations are smaller than the experimental errors. As mentioned in the discussion part, for the measurement of very fast exchanging water molecules, the mixing time should be reduced. This will also reduce the above mentioned problems with the back transfer, which allows to use the initial rate approximation for those short mixing times.

Equation 7, which describes the build-up of the cross peak volume for method II, can be derived by replacing M_b in eq A2 by eq A13, which is the decay of the bulk water magnetization during the application of the gradients:

$$M_b = M^0 \exp\left(-k_b\left(T_G - \frac{\delta_g}{3}\right)\right) \quad (\text{A13})$$

T_G is the time between the start of the first gradient and the start of the second one. Solving the differential equations in eq A2 and A1 yields eq 7 in the text. For method 2 the diffusion of the protein during the application of the gradients can be neglected.

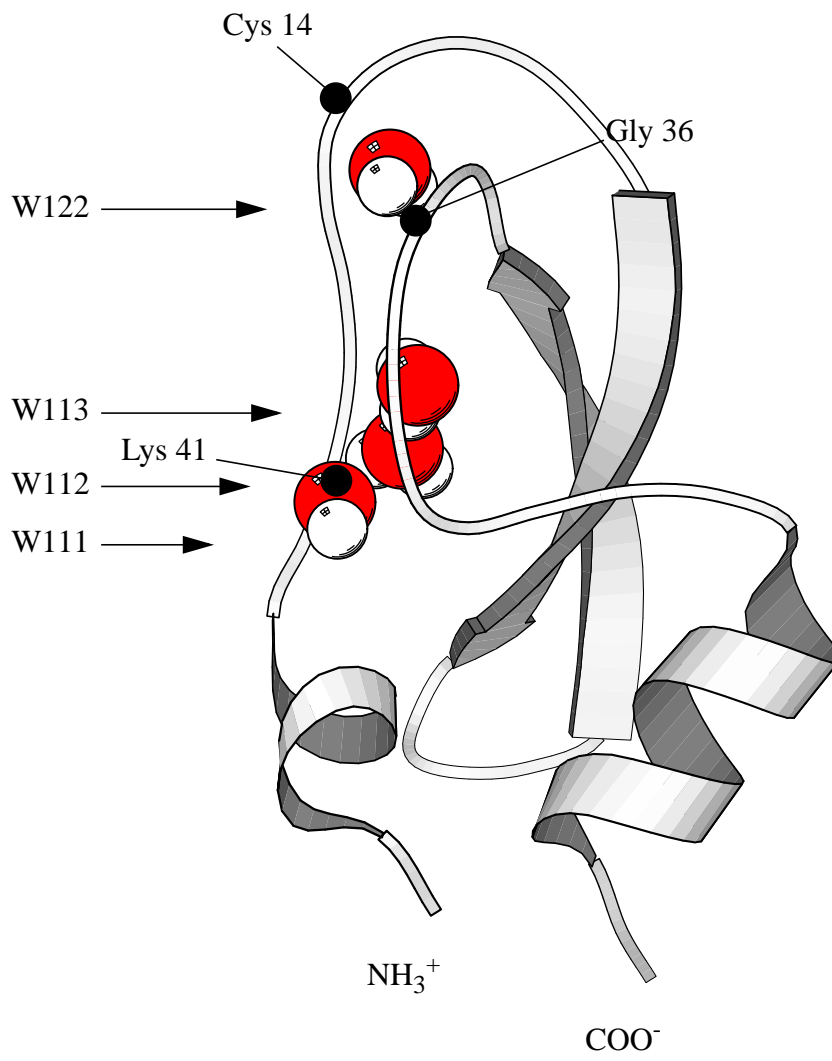


Figure 1

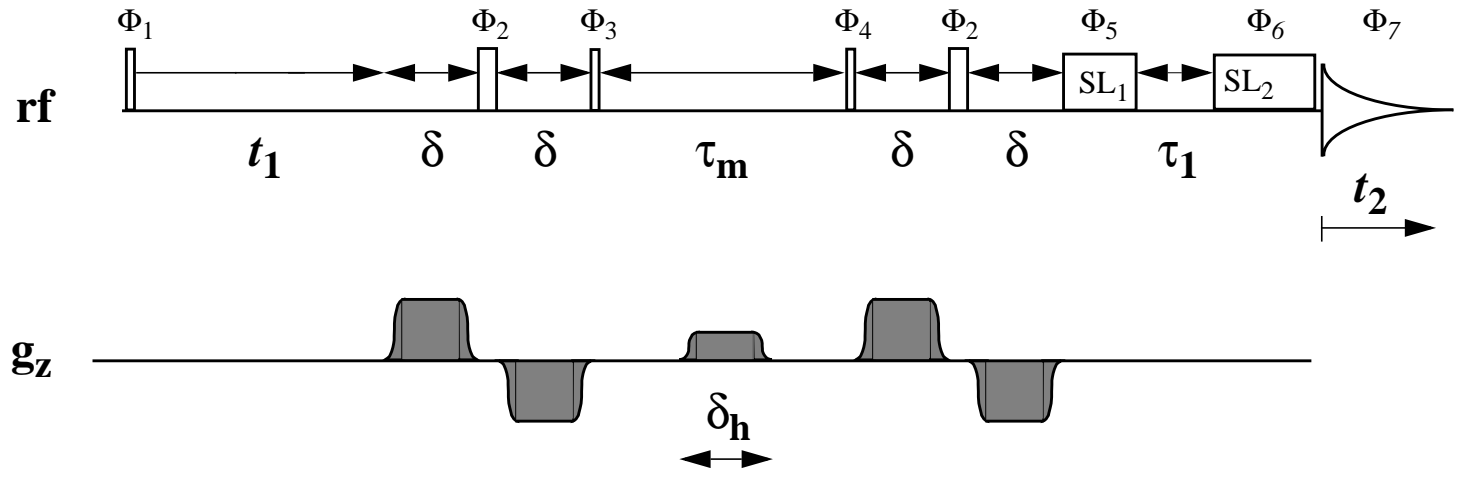


Figure 2

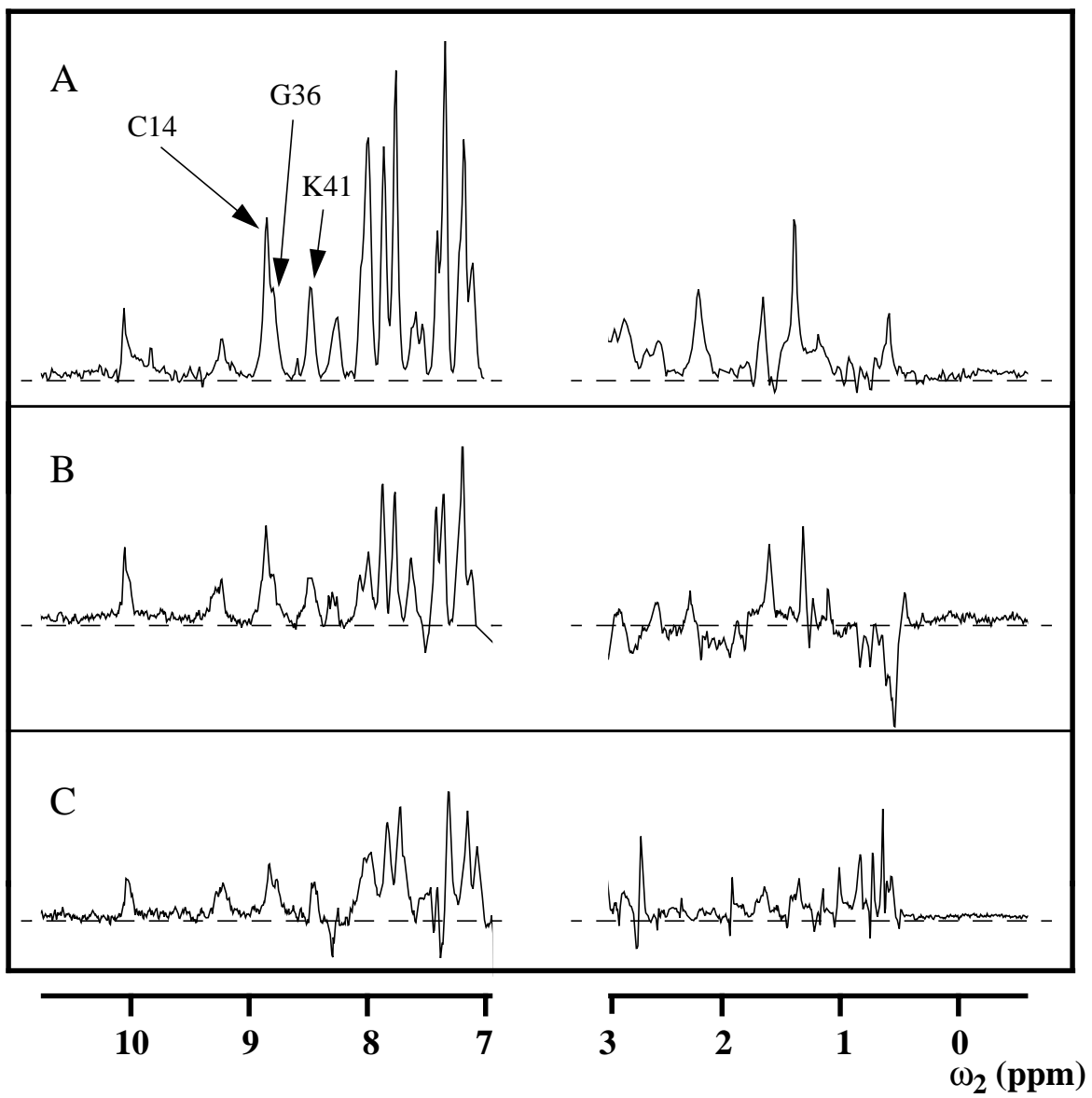


Figure 3

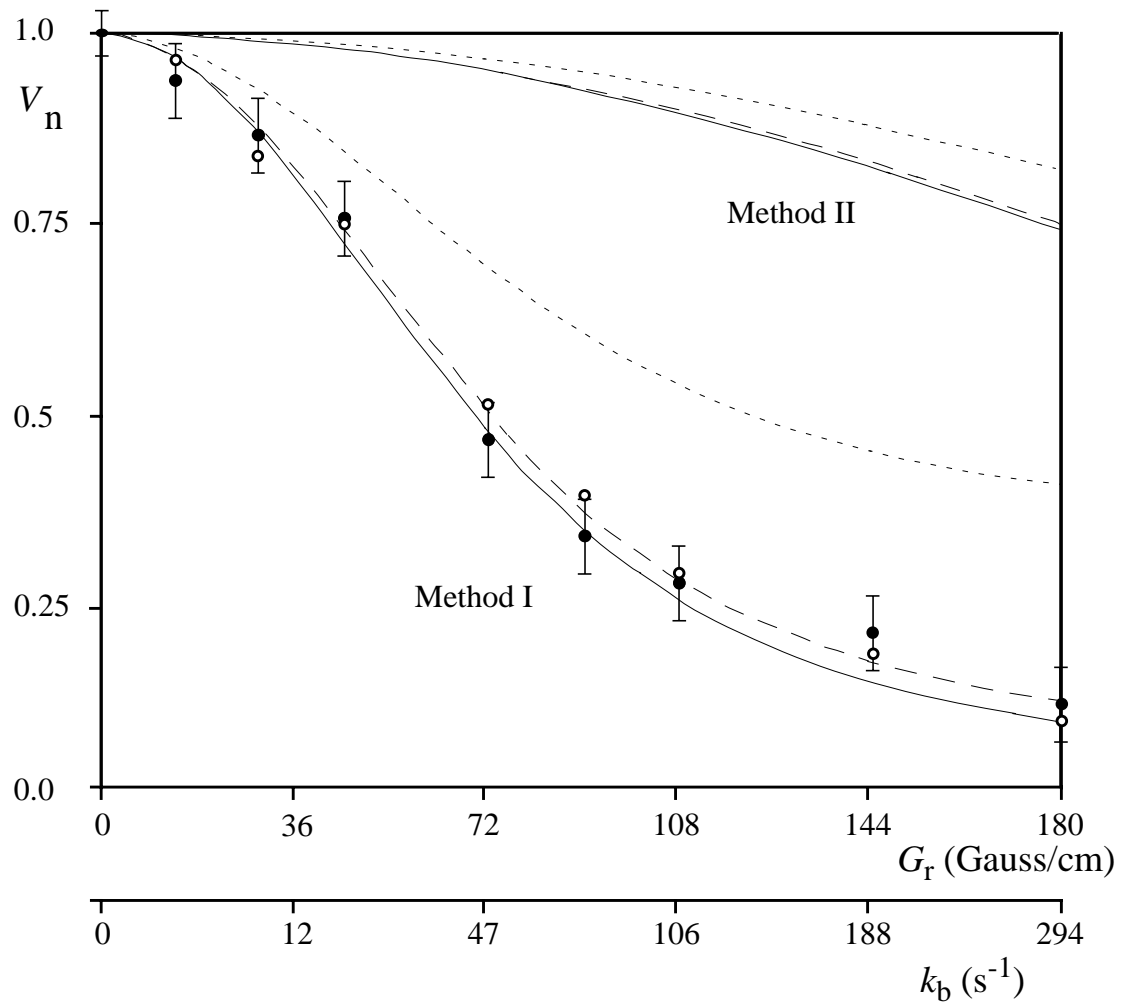


Figure 4

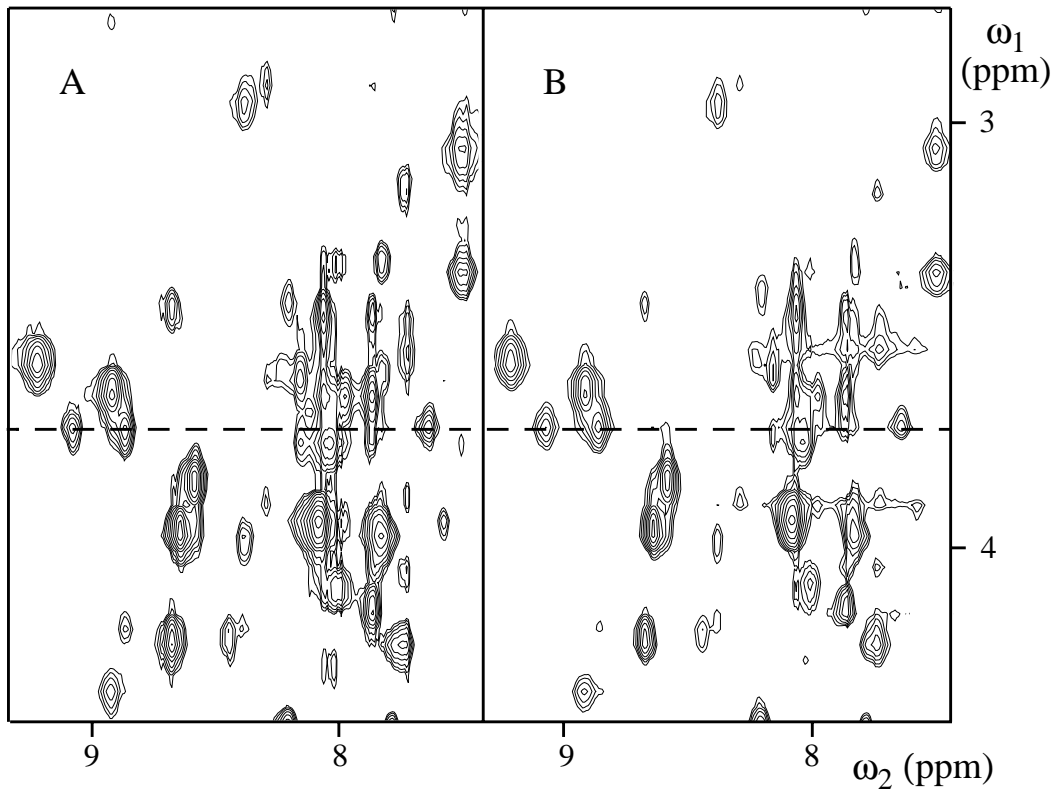


Figure 5

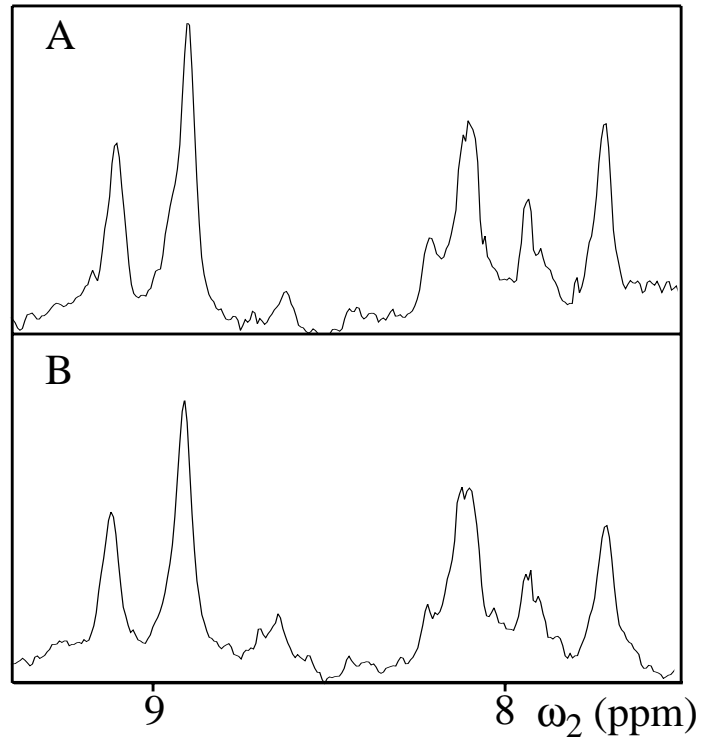


Figure 6

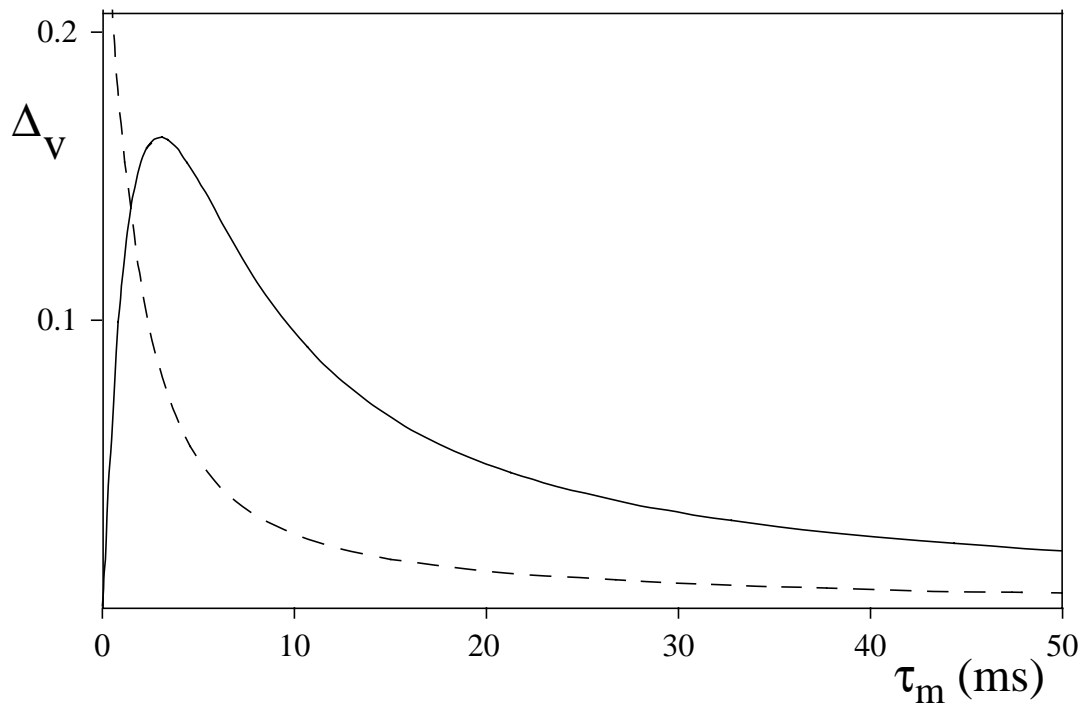


Figure 7